arXiv:cond-mat/0412313v1 [cond-mat.str-el] 13 Dec 2004

# Magnetic Phase Diagram of the Hole-doped $Ca_{2-x}Na_xCuO_2Cl_2$ Cuprate Superconductor

K. Ohishi,[1,*] I. Yamada,[2] A. Koda,[1] W. Higemoto,[1,†] S.R. Saha,[1]
R. Kadono,[1,‡] K.M. Kojima,[3] M. Azuma,[2,4] and M. Takano[2]

[1] *Institute of Materials Structure Science, High Energy Accelerator Research Organization (KEK), Tsukuba, Ibaraki 305-0801, Japan*
[2] *Institute for Chemical Research, Kyoto University, Uji, Kyoto 611-0011, Japan*
[3] *Department of Physics, Graduate School of Science, University of Tokyo, Bunkyo-ku, Tokyo 113-0033, Japan*
[4] *PRESTO, Japan Science and Technology Corporation (JST), Kawaguchi, Saitama 332-0012, Japan*

(Dated: March 23, 2022)

We report on the magnetic phase diagram of a hole-doped cuprate $Ca_{2-x}Na_xCuO_2Cl_2$, which is free from buckling of $CuO_2$ planes, determined by muon spin rotation and relaxation. It is characterized by a quasi-static spin glass-like phase over a range of sodium concentration ($0.05 \leq x \leq 0.12$), which is held between long range antiferromagnetic (AF) phase ($x \leq 0.02$) and superconducting phase where the system is non-magnetic for $x \geq 0.15$. The obtained phase diagram qualitatively agrees well with that commonly found for hole-doped high-$T_c$ cuprates, strongly suggesting that the incomplete suppression of the AF order for $x > 0.02$ is an essential feature of the hole-doped cuprates.

PACS numbers: 74.25.Ha, 74.72.-h, 76.75.+i

Since the discovery of high-$T_c$ superconductivity, the magnetic phase diagram of layered $CuO_2$ materials as a function of carrier doping has been one of the key issues directly related to the mechanism of superconductivity. It is known that while all insulating parent compounds of the planar cuprate superconductors exhibit long range antiferromagnetic (AF) order below a well-defined temperature ($T_N$), insulator-to-metal transition and associated suppression of the AF order occurs when they are subjected to carrier doping. A copper oxychloride $Ca_{2-x}Na_xCuO_2Cl_2$ (Na-CCOC) [1, 2] is a model system for studying lightly doped states of the single $CuO_2$ plane. This superconductor with the maximum $T_c$ = 28 K at $x \sim 0.2$ can be derived from the prototypical high-$T_c$ superconducting material, $La_{2-x}Sr_xCuO_4$ (LSCO), by replacing lanthanum (strontium) atoms by calcium (sodium) and the oxygen atoms at the apices of $CuO_6$ octahedra by chlorine. Recently, it draws much attention due to their unique character that the crystal structure is free from any distortion down to the lowest temperature [3]. Moreover, excellent cleavability of the single crystals [4] enabled investigations of the electronic state in lightly doped $CuO_2$ planes by surface sensitive measurements such as angle resolved photoemission spectroscopy (ARPES) and scanning tunneling microscopy and spectroscopy (STM/STS).

According to the results of ARPES measurements on a superconducting specimen ($x = 0.1$), the band dispersion is a consequence of the valence band of the parent insulator shifting to the chemical potential in accordance with the hole doping [5]. The resulting fingerprints of the parent insulator manifest themselves in the form of a shadow band and a large pseudogap. These results are remarkably different from the prevailing picture proposed for the prototypical high-$T_c$ superconducting material LSCO, where the chemical potential remains fixed while new states are created around it by doping. It is speculated that these differences between Na-CCOC and LSCO may be due to the difference of apical site and associated distortion of $CuO_2$ planes. More interestingly, the real space imaging of underdoped Na-CCOC ($0.06 \leq x \leq 0.12$) by the STM/STS has revealed that there are nanoscale inhomogeneity in the electronic structure with a characteristic scale of 4–5 times the lattice constant [6] and also checkerboard-like electronic crystal, suggesting the coexistence of superconductivity and charge ordering [7]; it must be noted that such measurements for underdoped cuprates have become possible for the first time in Na-CCOC. Meanwhile, little is known on the magnetic property of Na-CCOC except for the parent compound ($x = 0$) [3], since it is hard to prepare large samples for neutron measurements and to detect the susceptibility by SQUID. Thus, it would be of great interest, particularly over the underdoped region, to clarify the ground state property of Na-CCOC in terms of magnetism.

In this Letter, we report on the magnetic phase diagram of Na-CCOC ($0 \leq x \leq 0.20$) determined by muon spin rotation and relaxation ($\mu$SR) measurements. We have observed clear muon spin precession signals in the lightly doped samples ($x \leq 0.02$), indicating the appearance of a long range AF order. While no precession signal was identified in those with $0.05 \leq x \leq 0.12$, evidence was found for a quasi-static spin glass(SG)-like state at lower temperatures. It suggests a general trend that the suppression of long range AF order is strong

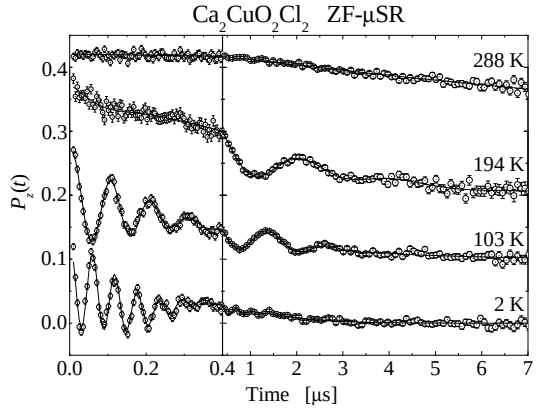



FIG. 1: ZF-$\mu$SR time spectra, $P_z(t)$, in CCOC at various temperatures. The left and right column corresponds to $P_z(t)$ for 0–0.4 $\mu$s and 0.4–7 $\mu$s, respectively. Note that $P_z(t)$ values of 288 K and 194 K are added 0.2, and that of 103 K is added 0.1.

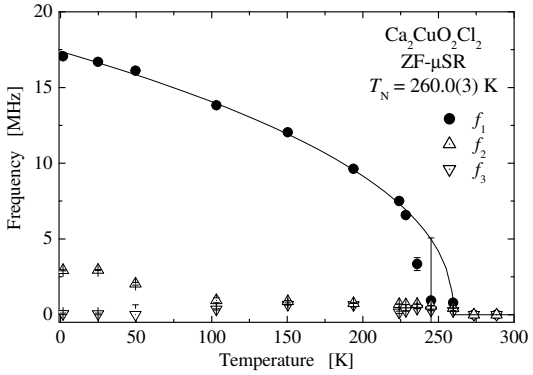



FIG. 2: Temperature dependence of the muon spin precession frequencies in CCOC. Solid curve is a fitting result for the data $f_1$ by a form $A(T_{\rm N} - T)^{\gamma}$, where $T_{\rm N}$ = 260.0(3) K is obtained.

but incomplete over the relevant range of sodium concentration. In particular, the present result is the first example for a good correspondence between such an inhomogeneous magnetic state and the nanoscale electronic inhomogeneity revealed by STM/STS [6]. Moreover, the obtained magnetic phase diagram resembles those of the hole-doped high-$T_{\rm c}$ cuprates [8], supporting the universality of the present phase diagram which is important for the basic understanding of the hole-doped cuprates.

The Na-CCOC compounds used in this study were synthesized under high pressure [1, 2]. The samples were characterized by means of magnetization and powder X-ray diffraction. The lattice parameters were determined by using a Rietveld analysis for all samples in order to evaluate the sodium concentration dependence of the lattice parameters. Zero field (ZF)-$\mu$SR measurements were conducted at TRIUMF and at the Muon Science Laboratory, High Energy Accelerator Research Organization (KEK-MSL). We prepared eleven sets of Na-CCOC polycrystalline specimens, $x$ = 0, 0.0025, 0.005, 0.01, 0.02, 0.05, 0.07, 0.10, 0.12, 0.15, and 0.20, having a dimension of about 100 $\sim$ 250 mm$^2$ with $\sim$ 1 mm thickness. These samples were mounted on a thick sample holder (KEK-MSL) or on a thin sheet of mylar film (TRIUMF, where one can obtain background free spectra) and loaded to the $^4$He gas flow cryostat. ZF-$\mu$SR measurements were mainly performed at temperatures between 2 K and room temperature, and additional measurements were performed at ambient temperature under a transverse field ($\simeq$ 2 mT) to calibrate the instrumental asymmetry. The dynamics of local magnetic fields at the muon sites was investigated by longitudinal field (LF)-$\mu$SR measurements [9].

Figure 1 shows the time spectra of the muon spin polarization $P_z(t)$ observed in non-doped CCOC under zero field at typical temperatures, where muon spin precession signals are clearly observed below $T_{\rm N} \simeq$ 260 K. These signals unambiguously demonstrate that the system falls into a long range AF state below $T_{\rm N}$. Consequently, the data were analyzed by the following function; $P_z(t) = \sum_{i=1}^{n} A_i \exp[-(\sigma_i t)^2] \cos(2\pi f_i t + \phi) + A_{\rm n} \exp[-(\sigma_{\rm n} t)^{\beta}]$, where $A_i$ and $A_{\rm n}$ are the asymmetry of oscillating and non-oscillating components, $f_i$ is the muon spin precession frequency, $\sigma_i$ and $\sigma_{\rm n}$ are the relaxation rate, $\beta$ is the power of the exponent. The relevant spectra taken at TRIUMF were free from background.

The temperature dependence of $f_i$ is shown in Fig. 2. It exhibits a sharp reduction towards 260 K, where the oscillating component disappears around 275 K. This is consistent with the previous neutron result in which Bragg peak appears below $T_{\rm N}$ = 247(5) K [3]. As shown in Fig. 1 and Fig. 2, two different frequencies are observed below 260 K, and one of which exhibits further splitting into two components below around 100 K. It is interesting to note that one of those components ($f_2$) takes a value common to that in LSCO ($\sim$ 5 MHz) [10, 11, 12], and $f_1$ seems to be common to that in $Sr_2CuO_2Cl_2$ (SCOC) [13]. The data of $f_1$ are well reproduced by a function of the form $A(T_{\rm N} - T)^{\gamma}$, with $T_{\rm N}$ = 260.0(3) K and $\gamma$ = 0.44(1).

While clear muon spin precession signals were observed in those with small $x$, $T_{\rm N}$ showed a steep decrease with increasing sodium concentration. A fit procedure similar to that for CCOC has been applied to the data in the Na-doped samples ($0 < x \leq 0.02$). The splitting of frequency from two to three components below around 100 K were commonly observed in the samples with $x$ = 0.0025 ($T_{\rm N}$ = 240.6(8) K) and 0.005 ($T_{\rm N}$ = 185.3(1.3) K). On the other hand, there remained only two components below $T_{\rm N}$ in $x$ = 0.01 ($T_{\rm N}$ = 34.5(3)K) and 0.02 ($T_{\rm N}$ = 6.6 K).

Figure 3 shows the ZF-$\mu$SR time spectra in a specimen with $x$ = 0.05 at various temperatures. As shown in the inset, no muon spin precession signal was observed at the lowest temperature ($T$ = 2 K). It clearly indi-

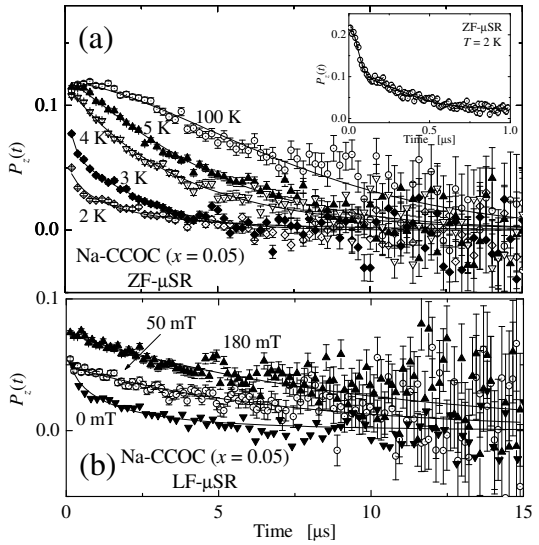



FIG. 3: (a) ZF-$\mu$SR time spectra in Na-CCOC with $x = 0.05$ at various temperatures. The inset shows a ZF-$\mu$SR time spectrum at 2 K where no spontaneous precession signal is observed. (b) LF-$\mu$SR time spectra at 2 K under various applied fields. $P_z(t)$ was obtained by subtracting the temperature-independent contribution from the silver sample holder.

cates that a strongly disordered magnetic ground state dominates over the AF long range order at this sodium concentration. The depolarization is well described by $P_z(t) = A_1 \exp(-\lambda_1 t) \exp[-(\Delta t)^2] + A_2 \exp(-\lambda_2 t) + A_{\rm B}$, where $A_i$ is the decay asymmetry for signals from the sample, $A_{\rm B}$ is that from the sample holder, $\lambda_i$ is the relaxation rate, and $\Delta$ is the *nuclear* dipolar width predominantly determined by $^{63,65}$Cu and $^{35,37}$Cl nuclear moments (see below). The values of $\Delta$ were fixed to those determined at ambient temperature where $\lambda_i \simeq 0$. The second term is needed only below 3 K. Solid curves in Fig. 3(a) are the fit results. It was revealed that while $\lambda_1$ is almost independent of temperature above 6 K, it starts to increase rapidly with decreasing temperature below 6 K. Such fast relaxation without any detectable oscillation is a common signature of disordered magnetism which is either static or dynamically fluctuating. The two possibilities can be discriminated by the field dependence of $\lambda_i$ under a LF. Figure 3(b) shows the LF-$\mu$SR time spectra at 2 K under various magnetic fields ($x = 0.05$). It is clear from the analysis that considering the effect of LF, the relaxation rate remains almost unchanged with increasing field from 50 to 180 mT, strongly suggesting that the local field probed by muons is fluctuating due to the slowing down of electronic Cu moments. The fluctuation rate becomes slow enough below 6 K where $\lambda_1$ starts to increase, where $\lambda_1 \simeq (\gamma_\mu A_\mu)^2/\nu \sim 10^5$ s$^{-1}$ with $\gamma_\mu A_\mu \simeq 2\pi f_1 (T \to 0)$. Here, $\gamma_\mu$ is the muon gyromagnetic ratio ($= 2\pi \times 135.54$ MHz/T). This leads to an estimation for the fluctuation rate, $\nu \sim 10^9$ s$^{-1}$ at 2 K. We made additional measurements using a $^3$He–$^4$He dilution refrigerator in the specimen with $x = 0.10$ and found that a quasi-static SG-like state is realized below $\sim 0.6$ K. This indicates that the increase of $\lambda_i$ is a precursor of a SG-like transition; the temperature region over which the fluctuation is observed is much wider than that associated with the AF transition for $x \leq 0.02$. Thus, we define the onset of SG-like behavior at $T_{\rm D} \sim 6$ K in $x = 0.05$ specimen. A similar behavior in both ZF-$\mu$SR and LF-$\mu$SR was observed for $x = 0.07$, 0.10 and 0.12, where $\lambda_1$ increases below $T_{\rm D} \sim 4.3$ K, 3.5 K and 2.5 K, respectively.

The superconducting character of the present samples is examined by the temperature dependence of the magnetic susceptibility, as shown in the inset of Fig. 4 for $x = 0.10$, 0.12, 0.15 and 0.20. A clear sign of the Meissner effect is observed in the samples with $x = 0.12, 0.15$ and 0.20, while no bulk superconductivity is detected for $x = 0.10$. From these data, the superconducting volume fraction was estimated to be 1%, 16%, 60% and 48% in the respective samples with $x = 0.10$, 0.12, 0.15 and 0.20. Since the volume fraction is very small in those with $x = 0.10$ and 0.12, it is reasonable to presume a phase separation in those samples with the superconducting phase as a minority phase.

ZF-$\mu$SR time spectra in the specimen with $x = 0.15$ and 0.20 exhibit the least temperature dependence down to 2 K. The relaxation is predominantly due to static and randomly oriented nuclear magnetic moments which give rise to depolarization described by the Kubo-Toyabe function, $G_{\rm KT}(t)$. It is characterized by a Gaussian decay, $\sim \exp[-(\Delta t)^2]$, at early times followed by a recovery of the asymmetry to 1/3, where $\Delta$ is the rms width of the field distribution arising from the nuclear moments. Besides the signature of these static nuclear magnetic moments, we obtained no evidence for any kind of additional magnetic moments in the specimen with $x = 0.15$ and 0.20. The only exception is that the spectrum obtained at 2 K seems to exhibit a tiny enhancement of relaxation compared with that at 171 K. Considering this point, the data were analyzed by the following function, $P_z(t) = A G_{\rm KT}(t) \exp(-\Lambda t) + A_{\rm B}$ , which yields $\Delta = 0.154(20)$ $\mu$s$^{-1}$ ($x = 0.15$) and $0.162(8)$ $\mu$s$^{-1}$ ($x = 0.20$). Although $\Lambda$ ($\sim 10^{-2}$ $\mu$s$^{-1}$) slightly depends on temperature, it may be attributed to a slow dynamics of muon (e.g., diffusion). Another possibility is that $P_z(t)$ may be a sum of $G_{\rm KT}(t)$ with different values for $\Delta$ due to multiple muon stopping sites with varying distance to the Cu and Cl nuclear moments (see below). As a summary of our results, the magnetic phase diagram of Na-CCOC as a function of $x$ is shown in Fig. 4.

Since the electronic Cu moment is the only source of strong local magnetic fields ($\gg 1$ mT) in the AF phase, the observation of multiple components in the precession signals for $x \leq 0.02$ suggests that there are multiple muon sites in Na-CCOC. In the case of ZF-$\mu$SR, muons experience a local field $\boldsymbol{H}_{loc} = \boldsymbol{H}_{dip} + \boldsymbol{H}_{fc}$, where

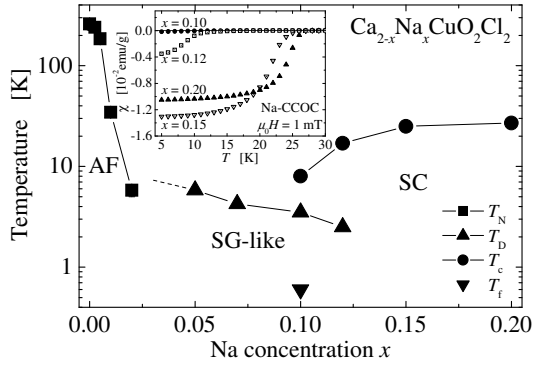



FIG. 4: Magnetic phase diagram of Na-CCOC. The transition temperature for the SG-like state ($T_{\rm D}$) is defined as an onset temperature where the spin fluctuation rate becomes lower than $10^9$ s$^{-1}$. The spin freezing temperature ($T_{\rm f}$) is only defined in $x = 0.10$ specimen. The inset shows the temperature dependence of magnetic susceptibility measured for ($x = 0.10$, 0.12, 0.15 and 0.20) in an applied field $\mu_0 H = 1$ mT after field-cooling process.

$\boldsymbol{H}_{dip} = \sum_i (3r_i^\alpha r_i^\beta / r_i^2 - \delta_{\alpha\beta})/r_i^3$ $(\alpha, \beta = x, y, z)$ is the magnetic dipolar field from the $i$-th $Cu^{2+}$ ion at a distance $r_i$ from the muon, and $\boldsymbol{H}_{fc}$ is the Fermi-contact hyperfine field due to the finite electron spin density at the muon site. Since the latter is likely to be negligible as in the case of $La_2CuO_4$ (LCO), we can calculate the local field at a muon site as the sum of magnetic dipolar field from the Cu moments with their moment size $\simeq 0.25(10)\mu_{\rm B}$ as determined by neutron diffraction [3]. Another source of information is the nuclear dipolar width $\Delta$ determined in the paramagnetic state. In the case of polycrystalline samples, $\Delta$ is determined by the second moment, $\Delta^2 = \frac{5}{3}\gamma_\mu^2 \overline{\sigma_{\rm VV}^2} = \frac{4}{9}\gamma_\mu^2 \sum_i \overline{\mu_i^2 \frac{1}{r_i^6}}$, where $\sigma_{\rm VV}$ is a value defined by Van Vleck [14] and $\mu_i$ is the *nuclear* magnetic moment situated at distance $r_i$ from the muon site. Comparison of the experimental values of $H_{\rm dip}$ and $\Delta$ with those calculated by the above formulae yields $R_1 = 1.97$Å (from $f_1$) and $R_2 = 3.52$Å (from $f_2$), respectively. Considering the distance of $r_{\rm Cu-O} = 1.934$Å in $CuO_2$ plane and $r_{\rm Cu-Cl} = 2.737$Å in CCOC, we conclude that $f_1$ and $f_2$ respectively correspond to the muons stopped near the planer oxygens and apical chlorines. The latter site is close to that in LCO, which is perfectly in line with the fact that $f_2$ is close to that observed in LCO. The above conclusion is also consistent with a theoretical estimation made for LCO [15], where muons are predicted to be attracted by the negative charge at the apical oxygen atoms. The appearance of additional site for CCOC may be explained by the reduced ionic charge of $Cl^-$, which makes the site near the apical Cl less attractive to muons compared with that near $O^{2-}$ in terms of the electrostatic energy. Then it seems reasonable that a considerable fraction of implanted muons dwells on the $CuO_2$ plane containing $O^{2-}$ ions.

The revelation of SG-like phase in the underdoped Na-CCOC is one of the most important results in the present study. As mentioned earlier, the very recent STM/STS measurements on the corresponding specimen have revealed a nanoscale inhomogeneity in the electronic density of state (DOS) [6]. Considering that the SG-like state is observed as a bulk majority over the region $0.05 \leq x \leq 0.12$, it is natural to presume that the quasi-static SG-like state (magnetic inhomogeneity) has a close link with the electronic inhomogeneity observed in the underdoped Na-CCOC. However, the possibility to interpret the inhomogeneity as those consisting of the AF domains is ruled out; it would lead to the spontaneous muon precession with an amplitude proportional to the volume fraction of AF domains [16]. Accordingly, the low DOS area probed by STS/STM should not be interpreted simply as the AF domains. The picture of diluted local moments would be also inconsistent with the STM/STS observation, since such moments would not induce the nanoscale inhomogeneity. Thus, one of the few possibilities to explain both $\mu$SR and STM/STS results would be to consider a spin density wave (SDW) associated with the DOS distribution. We point out that the observed time spectrum shown in the inset of in Fig. 3(a) exhibits a close resemblance with that in the SDW state [17]. The sensitivity to induce such an inhomogeneity upon the hole-doping would be a key to understand the electronic state of $CuO_2$ planes. We also note that no strong anomaly was observed for $x = 0.12$ ($\simeq 1/8$), suggesting either the buckling of $CuO_2$ planes or the ionic radius of alkaline metals (Ca<Sr<Ba) may be related to the 1/8 anomaly.

The remaining issue is the splitting of frequency below 100 K. In the case of SCOC, it is also reported that the muon precession frequency splits into two components below 60 K [13], which is attributed to an intrinsic effect of possible spin reorientation. Accordingly, one possible scenario is that a similar spin reorientation may occur also in CCOC. However, it turns out that both neutron and magnetization measurements report no sign of such spin-flop transition in CCOC [3]. The fact that $f_1$ remains unique below 100 K also disfavors this scenario. Another possibility is that muons near the apical Cl ions may undergo a local site change below 100 K, although the origin of the instability is unclear at this stage.

We would like to thank the staff of TRIUMF and KEK for their technical support during the experiments. This work was partially supported by a Grant-in-Aid for Creative Scientific Research and a Grant-in-Aid for Scientific Research on Priority Areas by Ministry of Education, Culture, Sports, Science and Technology, Japan.

* Electronic address: kazuki.ohishi@kek.jp
† Present Address: Advanced Science Research Center, Japan Atomic Energy Research Institute, Tokai, Ibaraki 319-1195, Japan
‡ Also at School of Mathematical and Physical Science, The Graduate University for Advanced Studies.

[1] Z. Hiroi, *et al.*, Nature (London) **371**, 139 (1994).
[2] Z. Hiroi, *et al.*, Physica C **266**, 191 (1996).
[3] D. Vaknin, *et al.*, Phys. Rev. B **56**, 8351 (1997).
[4] Y. Kohsaka, *et al.*, J. Am. Chem. Soc. **124** 12275 (2002).
[5] Y. Kohsaka, *et al.*, J. Phys. Soc. Jpn. **72**, 1018 (2003).
[6] Y. Kohsaka, *et al.*, Phys. Rev. Lett. **93**, 097004 (2004).
[7] T. Hanaguri, *et al.*, Nature **430**, 1001 (2004).
[8] Ch. Niedermayer, *et al.*, Phys. Rev. Lett. **80**, 3843 (1998).
[9] A. Schenck, *Muon Spin Rotation: Principles and Applications in Solid State Physics* (Adam Hilger, Bristol, 1986).
[10] Y.J. Uemura, *et al.*, Phys. Rev. Lett. **59**, 1045 (1987).
[11] Y.J. Uemura, *et al.*, Physica C **153-155**, 769 (1988).
[12] Y.J. Uemura, *et al.*, Hyp. Int. **49**, 205 (1989).
[13] L.P. Le, *et al.*, Phys. Rev. B **42**, 2182 (1990).
[14] R.S. Hayano, *et al.*, Phys. Rev. B **20**, 850 (1979).
[15] S.B. Sulaiman, *et al.*, Phys. Rev. B **49**, 9879 (1994).
[16] A.T. Savici, *et al.*, Phys. Rev. B **66**, 014524 (2002).
[17] K. Ohishi, *et al.*, J. Phys. Soc. Jpn. **69**, 2427 (2000).